ORIGINAL PAPER

Effect of High-Intensity Ultrasound on the Crystallization Behavior of High-Stearic High-Oleic Sunflower Oil Soft Stearin

Jaime A. Rincón-Cardona · Lina M. Agudelo-Laverde · María L. Herrera · Silvana Martini

Abstract The objective of this research was to evaluate the effect of high-intensity ultrasound (HIU) and crystallization temperature (T_c) on the crystallization behavior, melting profile, and elasticity of a soft stearin fraction of high-stearic high-oleic sunflower oil. Results showed that HIU can be used to induce and increase the rate of crystallization of the soft stearin with significantly higher SFC values obtained in the sonicated samples, especially at higher T_c. SFC values were fitted using the Avrami model, and higher k_n and lower n values were obtained when samples were crystallized with sonication, suggesting that sonicated samples crystallized faster and through an instantaneous nucleation mechanism. In addition, the crystal morphology, melting behavior, and viscoelasticity were significantly affected by sonication.

J. A. Rincón-Cardona
Escuela de Ciencia y Tecnología, Universidad Nacional de San Martín (UNSAM), Campus Miguelete, 25 de Mayo y Francia, 1650 San Martín, Provincia de Buenos Aires, Argentina
e-mail: rinconjarc@gmail.com

L. M. Agudelo-Laverde · M. L. Herrera
Facultad de Ingeniería, Instituto de Tecnología de Polímeros y Nanotecnología (ITPN), Consejo Nacional de Investigaciones Científicas y Técnicas (CONICET), 1428 Av. Las Heras 2214, Buenos Aires, Argentina
e-mail: magudelo@di.fcen.uba.ar

M. L. Herrera
e-mail: lidia@di.fcen.uba.ar

S. Martini (✉)
Department of Nutrition Dietetics and Food Sciences, Utah State University, 750 North 1200 East, 8700 Old Main Hill, Logan, UT 84322, USA
e-mail: silvana.martini@usu.edu

Introduction

High-intensity ultrasound (HIU) techniques use acoustic waves of very low frequency (between 20–100 kHz) to induce physical changes in materials. The food industry has shown interest in the use of this technique for several applications such as extraction, crystallization, homogenization, filtration, and emulsification [1, 2]. In particular, several research groups have employed this technology to change the crystallization behavior of edible lipids such as palm oil [3, 4], anhydrous milk fat [5–7], palm kernel oil [6], commercial shortenings [6, 8, 9], and cocoa butter [10]. Results from these studies showed that HIU can increase the crystallization rate, reduce crystal sizes, and induce the formation of stable polymorphic forms. These strong effects on crystallization behavior result in significant changes in the physical and functional properties of the lipids including increased hardness and elasticity as well as the formation of a crystalline network with sharper melting profiles.

High-stearic/high-oleic sunflower oil (HSHOSFO) is a new variety of sunflower oil recently developed in a collaborative effort between Spain and Argentina [11, 12]. This oil can be used in foods to increase their shelf life and to improve yields in industrial frying. Two main fractions can be obtained from this oil: a high-melting-point fraction, or hard stearin (HS), and a low-melting-point fraction, or soft stearin (SS) [13, 14]. A vast number of studies have been performed on the crystallization behavior of HS and SS fractions to characterize the physical properties of these new fats to be used as *trans* fat replacements. In

general, research has shown that HS behaves as a solid butter that could be employed for confectionery applications because of their particular triacylglycerol composition, where StOSt constitutes the higher proportion [14–18]. On the other hand, SS fractions could be used in applications such as spreads and fillings [13–18]. Some of these studies also showed that HS and SS fractions can crystallize in five different polymorphic forms: α, β′$_2$, β′$_1$, β$_2$, and β$_1$ [16–18], resulting in specific crystal morphologies and different functional and physical properties. Very little research has been performed on the effect that processing conditions have on the crystallization and physical properties of SS and HS fractions. One of the few studies was performed by Martini et al. [17], who evaluated the effect of agitation and crystallization temperature on the crystallization behavior of these systems. These authors report that in general a more stable polymorphic form is obtained in SS and HS samples crystallized with agitation at low supercoolings. In order to broaden the use of these new lipids in various food applications, it is important to understand how different processing conditions affect their crystallization behavior to optimize product quality and shelf life. Therefore, the objective of this research is to evaluate the effect of HIU on the crystallization behavior of the SS fraction of HSHOSFO and understand how these changes affect the physical and functional properties of the lipid network formed.

Experimental Procedures

Starting Material

A commercial fraction of soft stearin (melting point = 30.6 ± 0.1 °C—AOCS Method Cc 1-25) obtained by dry fractionation from HSHOSFO was employed in this work. The fatty acid chemical composition of the sample consisted of oleic acid (58.8 %), stearic acid (28.1 %), palmitic acid (5.3 %), and linoleic acid (3.0 %) [16–18].

Crystallization Methodology

Based on previous experiments [16–18], SS samples were crystallized at different temperatures (T_c = 17, 18, 19, 20 and 21 °C). This range of temperatures was chosen to evaluate different supercoolings: high supercoolings where the sample crystallizes just before T_c is reached and low supercoolings where samples crystallize several minutes after T_c is reached. Samples were melted in a microwave oven and then kept in an oven at 80 °C for 30 min to eliminate crystal history. The melted sample (10 g) was transferred to a double-walled crystallization cell connected to an external water bath that allowed for temperature control. This crystallization device was previously described in Martini et al. [5]. Samples were kept in the cell until sonication was applied (see section below) and then transferred to p-NMR tubes and a test tube using a 10-ml pipettor and placed in the water bath, which was set at T_c. Tubes were tempered at T_c in the water bath before the sample was transferred. The sample temperature was measured from the moment the sample was placed in the crystallization cell and throughout the entire experiment. Time zero was taken as the time when the sample reached T_c (9, 8, 7, 6, and 6 min for samples crystallized at 17, 18, 19, 20, and 21 °C, respectively). The crystallization behavior of the samples was followed as a function of time for 120 min. Crystal morphology and solid fat content were monitored during crystallization using a polarized light microscope and pulsed nuclear magnetic resonance equipment (p-NMR), respectively. Physical properties such as melting behavior and viscoelasticity were measured after 120 min of crystallization time.

HIU Application

HIU was applied to the samples when a slight turbidity was observed that indicated the presence of crystals. For samples crystallized at 17 °C, the first crystals were observed 2 min before the sample reached T_c; therefore, HIU was applied at that time ($t = -2$ min). For samples crystallized at 18, 19, 20, and 21 °C, crystals appeared after the samples reached T_c at $t = 3$, 8, 13, and 17 min, respectively. Therefore, HIU was applied at those time points. A Misonix Sonicator 3000 (Misonix Inc., Farmingdale, NY, USA) operating at a frequency of 20 kHz was used to apply the ultrasound pulse. A single treatment of HIU was applied to all samples that lasted for 10 s using a 5/64″-diameter microtip, which corresponds to a tip amplitude of 60 μm and an acoustic power of 0.5 W (17 W/cm^2).

Measurement of Solid Fat Content by p-NMR

A pulsed nuclear magnetic resonance (p-NMR) instrument (Bruker mq 20 Minispec, with a 0.47-T magnetic field operating at a resonance frequency of 20 MHz) was used to determine the solid fat content (SFC) of the samples. Samples were placed in NMR tubes (180 × 10 mm) and kept at T_c for 120 min as previously described. SFC values were determined as a function of time from $t = 0$ min up to 120 min. Duplicate runs were performed on consecutive days for each set of samples, and three tubes were measured in each run. SFC data collected as a function of time for each replicate were averaged, and the mean value was fitted to the Avrami equation (Eq. 1).

$$-\ln(1-f) = k_n \times t^n \tag{1}$$

where t is the time from the moment the sample reached T_c, k_n is the rate constant, f is the fractional extent of crystallization at any time, and n represents the index of the reaction. The fractional extent of crystallization can be expressed as the SFC at time t, divided by the maximum SFC obtained at a specific experimental condition (Eq. 2).

$$f = \frac{\text{SFC}}{\text{SFC}_{\text{max}}} \qquad (2)$$

The parameters k_n, n, and SFC_{max} were obtained from the fitted curves. Fitting was performed with Prism 6 (version 6.01, GraphPad Software Inc., La Jolla, CA, USA). A two-way ANOVA was performed to test for significant differences ($\alpha = 0.05$) for each parameter (k_n and n) as a function of sonication and T_c. The $t_{1/2}$ (time needed to reach half of the overall crystallization) was calculated from the fitted values of k_n and n using Eq. 3:

$$t_{1/2} = \left(\frac{\ln 2}{k} \right)^{1/n} \qquad (3)$$

Crystal Morphology by Polarized Light Microscopy (PLM)

The morphology of crystals obtained during crystallization was monitored using a polarized light microscope (Olympus BX 41, Olympus America Inc., Melville, NY, USA) equipped with a digital camera (Lumenera Infinity 2) and a controlled temperature platform. A drop of sample was taken from the test tube at different time points and placed in a thermostatized slide and cover slide. Pictures of crystals were taken as a function of time for 90 min. No pictures were taken between 90 and 120 min since no changes in crystal morphology were obtained at this stage.

Melting Behavior by DSC

The melting behavior of the crystallized samples was evaluated using a differential scanning calorimeter (DSC Q20, TA Instruments, New Castle, DE, USA). The instrument was calibrated with indium using a heating rate of 5 °C/min. After 120 min at T_c, 10–15 mg of the crystallized sample was taken from the test tube, placed in a hermetically sealed T_{zero} aluminum pan, and heated from T_c to 80 °C at 5 °C/min. An empty T_{zero} aluminum pan was used as a reference.

Viscoelastic Properties

The viscoelastic behavior for both sonicated and non-sonicated soft stearin was measured after 120 min of crystallization at T_c. Samples were taken from the test tube, transferred to the rheometer plate, which was thermostatized at T_c through a peltier system, and measured immediately.

A TA Instruments AR-G2 Magnetic Bearing Rheometer (TA Instruments, AR-G2, New Castle, DE, USA) was employed to evaluate the rheological properties of samples. Oscillatory tests were performed by a strain sweep test (2.9×10^{-4}; 10 % strain at 1 Hz of frequency) to obtain viscoelastic parameters such as tanδ, storage (G'), and loss (G'') moduli. The experiments were carried out using a parallel plate geometry (8-mm diameter, 1,000-μm gap). Temperature was maintained constant at the specific T_c throughout the measurement.

Statistical Analysis

All crystallization runs were performed in duplicate, and analytical measurements from each experimental replicate were performed in duplicate. Mean values and standard deviations are reported. Results were analyzed using two-way analysis of variance (ANOVA). The significance level was set at $\alpha = 0.05$, and multiple comparisons were performed using Tukey's test. Statistical analysis was carried out using Prism 6 (version 6.01, GraphPad Software Inc., La Jolla, CA, USA).

Results and Discussion

Measurement of Solid Fat Content by p-NMR

Figure 1 shows SFC values as a function of time for the SS sample crystallized with and without HIU at different T_c. As expected, the SFC increased over time in a sigmoidal manner, reaching a plateau for samples crystallized without HIU at low T_c ($T_c = 17$ and 18 °C). The crystallization behavior was significantly slower in the samples crystallized at higher T_c ($T_c = 19$, 20, and 21 °C); therefore, the plateau was not reached over the duration of the experiment (120 min). Higher SFCs were obtained at lower temperatures because of a higher supercooling. Values of 30.2 ± 0.3, 28.6 ± 0.7, 15.6 ± 3.6, 9.6 ± 3.0, and 4.9 ± 3.4 % were obtained at 120 min of crystallization for samples crystallized at 17, 18, 19, 20, and 21 °C, respectively, without HIU. A significant induction in the crystallization can be observed as a consequence of sonication for all T_cs evaluated. Higher SFC values were obtained as a consequence of sonication only during the first 15 and 45 min for samples crystallized at 17 and 18 °C, respectively (Fig. 1a, b). Sonication did not affect SFC values of samples crystallized at 17 and 18 °C after 20 and 60 min of crystallization, respectively. No significant differences were observed ($\alpha = 0.05$) between the SFC values of the sonicated and non-sonicated samples at 120 min with values of 31.6 ± 0.5 and 30.2 ± 0.4 % for samples crystallized at 17 and 18 °C, respectively. An induction in the onset of

Fig. 1 Solid fat content as a function of time of sunflower soft stearin without (*filled circle*) and with (*unfilled square*) HIU, crystallized at 17 °C (**a**), 18 °C (**b**), 19 °C (**c**), 20 °C (**d**), and 21 °C (**e**). SFC data are expressed as mean values and standard deviations of two replicates. Data were fitted using the Avrami equation for all sonicated samples and non-sonicated samples at 17 and 18 °C. The Avrami equation did not converge for data obtained for non-sonicated samples crystallized at 19, 20, and 21 °C
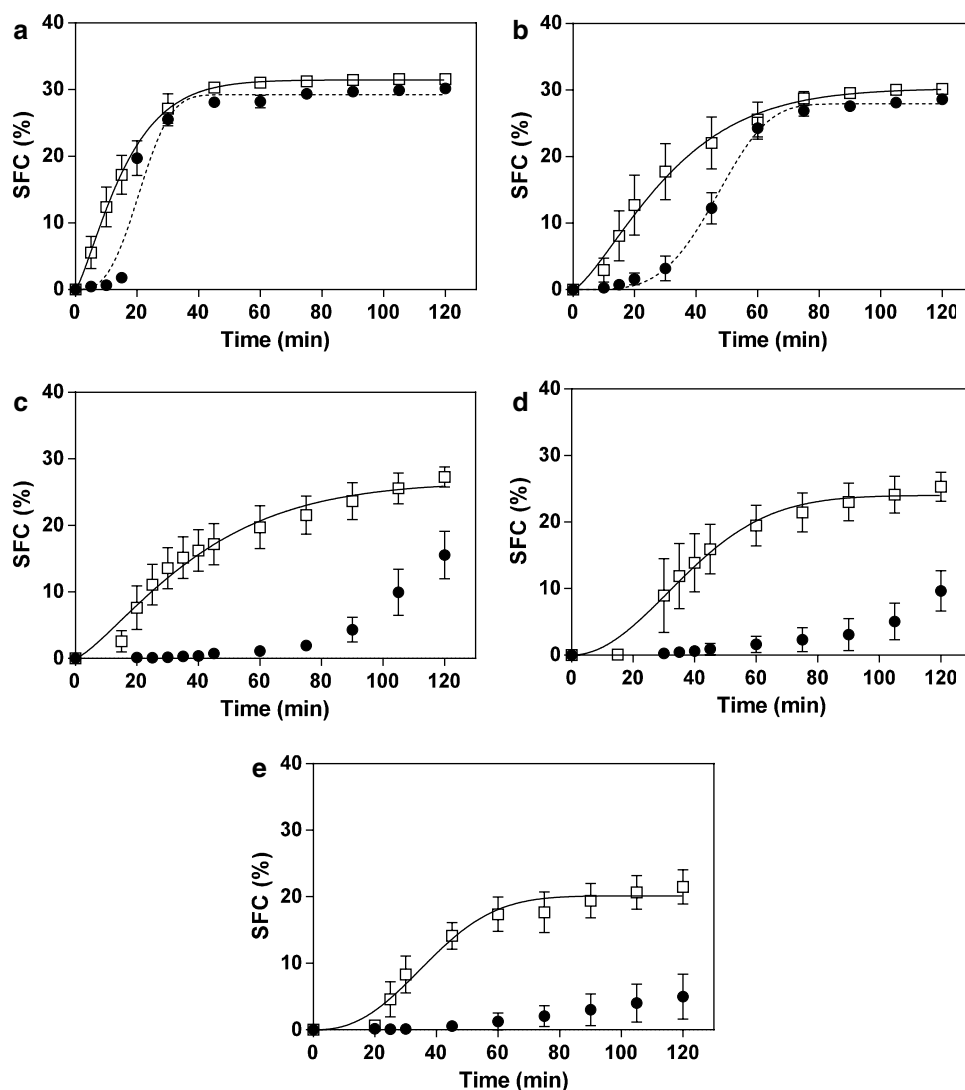
crystallization was more evident for samples crystallized at 19, 20, and 21 °C where SFC remained significantly higher ($\alpha = 0.05$) in sonicated samples even after 120 min of crystallization. It is important to note that sonicated samples crystallized at 19, 20, and 21 °C reached equilibrium before 120 min of crystallization time, showing a plateau in the SFC curve, while non-sonicated samples did not reach equilibrium even after 120 min (Fig. 1c–e). Values of non-sonicated samples crystallized at 19, 20, and 21 °C were 15.6 ± 3.6, 9.6 ± 3.0, and 5.0 ± 3.4 %, respectively, and 27.3 ± 0.5, 25.3 ± 2.2, and 21.5 ± 2.6 for the sonicated samples. An increase in the crystallization rate as a consequence of sonication was also reported by Chen et al. [4], who evaluated the SFC values as a function of time in palm oil samples crystallized at different T_c using different sonication conditions (power values between 47–475 W). However, power levels used in our study are significantly lower compared to the ones used by Chen et al.

The crystallization kinetics of the data reported in Fig. 1 were quantified using the Avrami equation (Eqs. 1, 2). Table 1 reports the k_n, n, SFC_{max}, $t_{1/2}$, and R^2 values of this fitting. K_n values decreased with increasing T_c, indicating a lower crystallization rate. This can be attributed to the lower supercooling generated during crystallization at higher temperatures. SFC values for samples crystallized without HIU at $T_c = 19$, 20, and 21 °C did not converge to the Avrami equation since the curves were not sigmoidal (Fig. 1). Significantly higher k_n values were obtained for samples crystallized at 17 and 18 °C with HIU compared to the ones obtained for the non-sonicated samples ($p < 0.05$). K_n values for the sonicated samples were three and four orders of magnitude higher than the ones obtained for the non-sonicated samples. This clearly shows a significant induction in the crystallization as a consequence of sonication and a faster crystallization rate. This induction in the crystallization rate was corroborated by the $t_{1/2}$ values obtained, with lower values reported for the sonicated

Table 1 Fitting parameters of the Avrami equation for SS samples crystallized at different T_c with and without HIU pulse

	T_c (°C)	k_n (min^{-n})	n	SFC$_{max}$ (%)	$t_{1/2}$ (min)	R^2
wo HIU	17	8.14×10^{-5}	2.98	29.3	20.8	0.9727
	18	1.60×10^{-7}	3.98	27.9	46.5	0.9912
	19	NA	NA	NA	NA	NA
	20	NA	NA	NA	NA	NA
	21	NA	NA	NA	NA	NA
w HIU	17	2.5×10^{-2}	1.28	31.5	13.1	0.9824
	18	8.0×10^{-3}	1.36	30.2	26.6	0.9445
	19	7.0×10^{-3}	1.31	26.5	33.4	0.8929
	20	5.0×10^{-4}	2.00	24.0	37.2	0.8729
	21	1.0×10^{-4}	2.45	20.1	34.4	0.9178

NA stands for "not applicable" and means that the data did not fit the Avrami model

samples (Table 1). SFC values obtained for the sonicated samples crystallized at $T_c = 19$, 20, and 21 °C were easily fitted to the Avrami equation with R^2 values between 0.8929 and 0.9178, indicating that the kinetics of these samples followed a sigmoidal shape (Fig. 1). As expected, k_n values for these samples decreased as T_c increased. These data show that HIU not only induces the onset of crystallization in the soft stearin, but also increases the crystallization rate. This effect is so significant that a similar crystallization rate is obtained in samples at 21 °C with HIU compared to the ones crystallized at 17 °C without HIU.

Table 1 also reports the Avrami exponent, n, which indicates the combined effect of nucleation and growth dimensionality [19]. T_c and HIU significantly affected the n values. Values increased with increased T_c and decreased with HIU application. Values of 3 and 4 were obtained for samples crystallized without HIU at 17 and 18 °C, respectively, suggesting disc-like or spherulitic growth, while n values of 1 were obtained for samples crystallized with HIU at 17, 18, and 19 °C, suggesting instantaneous nucleation and a rod-like growth. n values of 2 were obtained for samples crystallized with HIU at 20 and 21 °C, suggesting rod-like or disc-like growth with sporadic or instantaneous nucleation, respectively.

The induction in the crystallization kinetics and the reduction in n values observed in this study can be explained by the events created during sonication. Acoustic waves propagate in a liquid creating high- and low-pressure zones. When the acoustic pressure amplitude or acoustic intensity of these waves is greater than the static pressure, the liquid is put into tension, creating a cavity or void in the liquid. These cavities are filled with liquid vapor or any other gases dissolved in the liquid and grow into bubbles [20]. Depending on the acoustic intensity, frequency, and duration of the pulse, bubbles can either oscillate around their equilibrium position, a phenomenon known as stable cavitation, or the can grow and collapse. Bubble collapse is known as inertial cavitation, and this event is associated with very high and localized temperatures, pressures, and
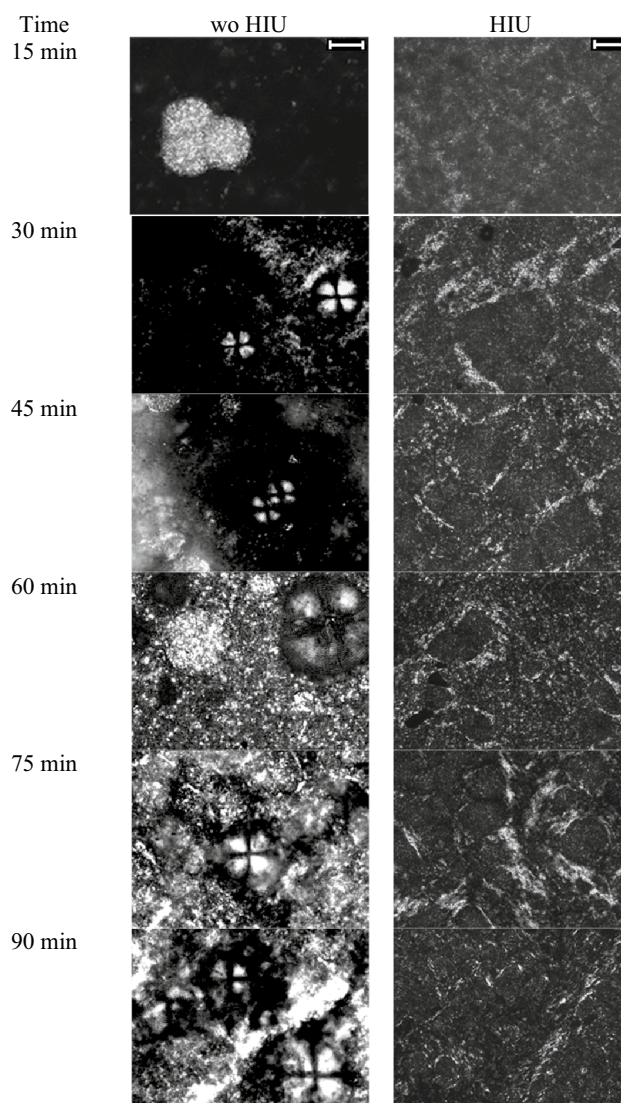

Fig. 2 Polarized-light microscopy (PLM) images of soft stearin crystallized at 17 °C without (wo HIU, *left column*) and with (HIU, *right column*) high-intensity ultrasound pulse. HIU pulse was applied at $t = -2$ min (2 min before the sample reached T_c). *White bar* in the first picture of *each column* represents 100 μm

shear forces. It is very likely that during sonication under the conditions used in this study, both stable and inertial cavitations are generated and directly affect the crystallization behavior of the lipid [21]. Stable cavities or bubbles can act as nuclei for new crystals to form, which will explain the reduction in *n* values obtained from the Avrami equation. In addition, inertial cavities can induce crystallization in several ways: (1) high localized shear forces created by bubble collapse can induce crystallization and can break existing crystals, generating more and smaller crystal clusters; (2) high localized pressures created by bubble collapse will generate a localized increase in the supercooling of the system, resulting in a faster crystallization rate. Even

though some research has been performed on monitoring bubble formation and cavitation events in oils [21], more research is needed in this area to fully understand the bubble dynamics in edible oils.

Crystal Morphology

Figures 2, 3, 4, 5, and 6 show the morphology of SS crystals obtained during the crystallization process when the samples were crystallized with and without the use of HIU at $T_c = 17, 18, 19, 20$, and 21 °C, respectively. As previously described, HIU was applied at the onset of crystallization
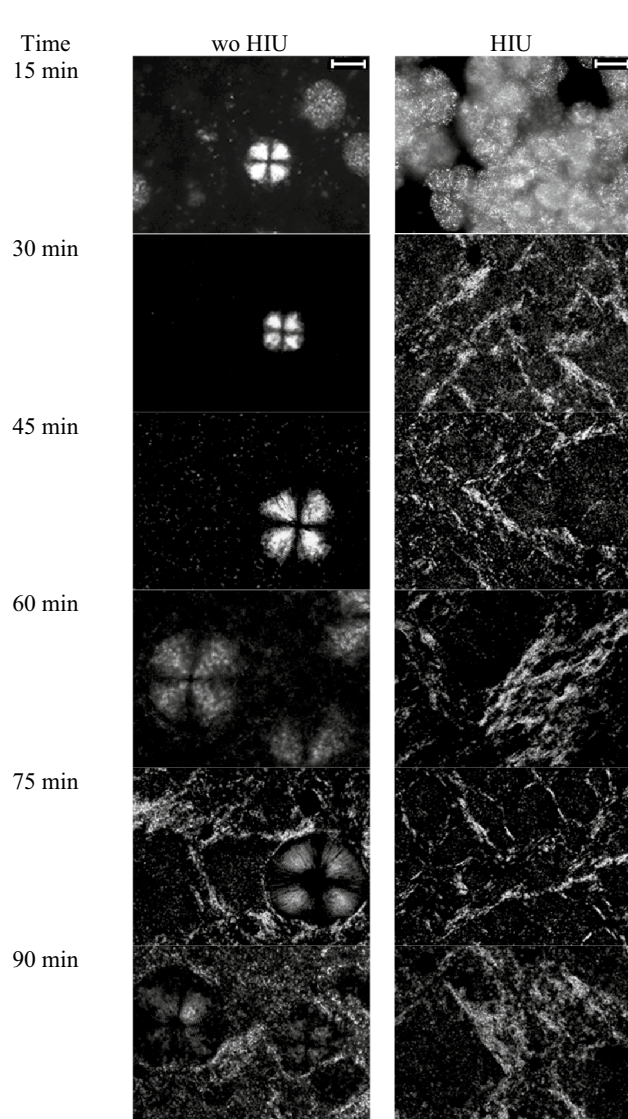
Fig. 3 Polarized-light microscopy (PLM) images of soft stearin crystallized at 18 °C without (wo HIU, *left column*) and with (HIU, *right column*) high-intensity ultrasound pulse. HIU pulse was applied at $t = 3$ min. *White bar* in the first picture of *each column* represents 100 μm
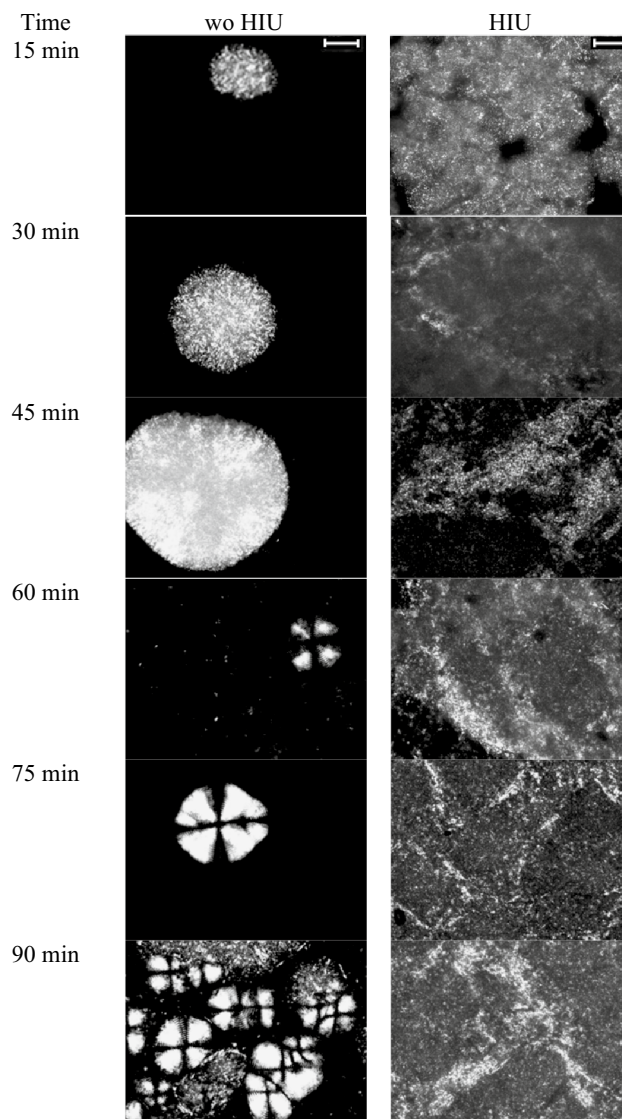
Fig. 4 Polarized-light microscopy (PLM) images of soft stearin crystallized at 19 °C without (wo HIU, *left column*) and with (HIU, *right column*) high-intensity ultrasound pulse. HIU pulse was applied at $t = 8$ min. *White bar* in the first picture of *each column* represents 100 μm

to allow for a better efficiency of the acoustic waves [8]. Therefore, HIU was applied 2 min before T_c was reached ($t = -2$ min) for samples crystallized at 17 °C and at $t = 3$, 8, 13, and 17 min for samples crystallized at 18, 19, 20, and 21 °C, respectively. The first column in these figures shows the morphology of crystals obtained when SS was crystallized without HIU as a function of time, and the second column shows the morphology of crystals obtained when the sample was crystallized with HIU. Different time points are shown in the rows of the figures. It is evident that HIU has a significant effect on crystal morphology, as shown in Figs. 2, 3, 4, 5, and 6, where sonicated samples

were characterized by agglomerated crystals with no evident microscopic organization, especially after the sample was kept at T_c for more than 30 min. Non-sonicated samples, on the other hand, were characterized by either ill-defined spherulites or by Maltese-cross-shaped crystals. It is very likely that the different morphologies observed correspond to different polymorphic forms. Rincon-Cardona et al. [16] studied the relationship between polymorphic forms and crystal shapes in SS samples and showed that ill-defined spherulites correspond to β'_2 polymorphs, while the Maltese-cross-shaped crystals correspond to a β_2 polymorph, and the agglomerate of crystals with no evident
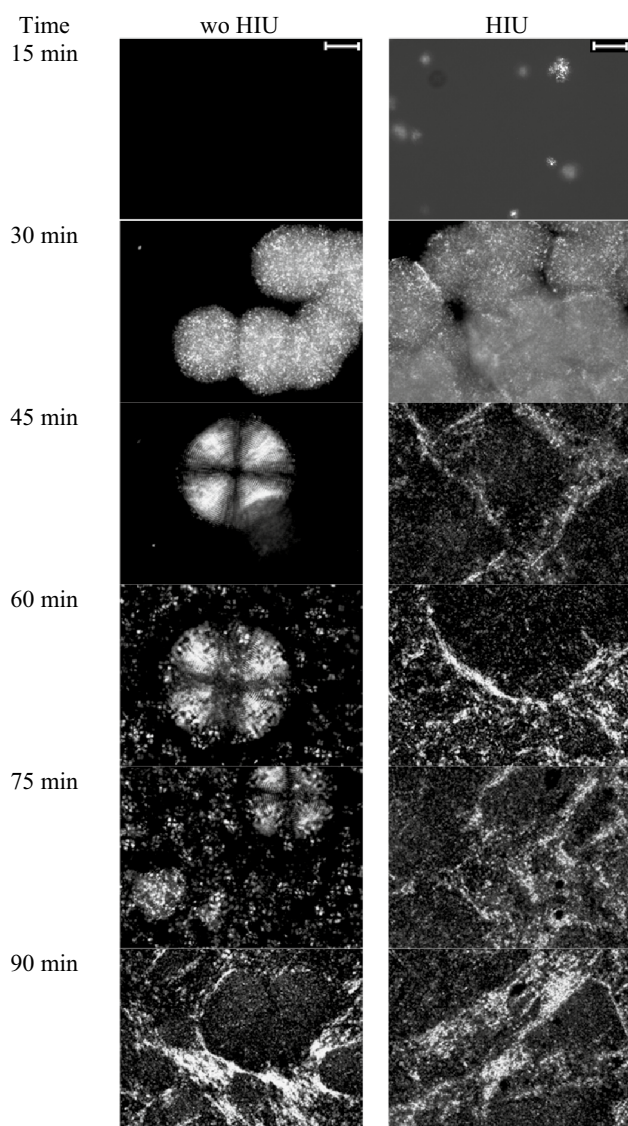
Fig. 5 Polarized-light microscopy (PLM) images of soft stearin crystallized at 20 °C without (wo HIU, *left column*) and with (HIU, *right column*) high-intensity ultrasound pulse. HIU pulse was applied at $t = 13$ min. *White bar* in the first picture of *each column* represents 100 μm
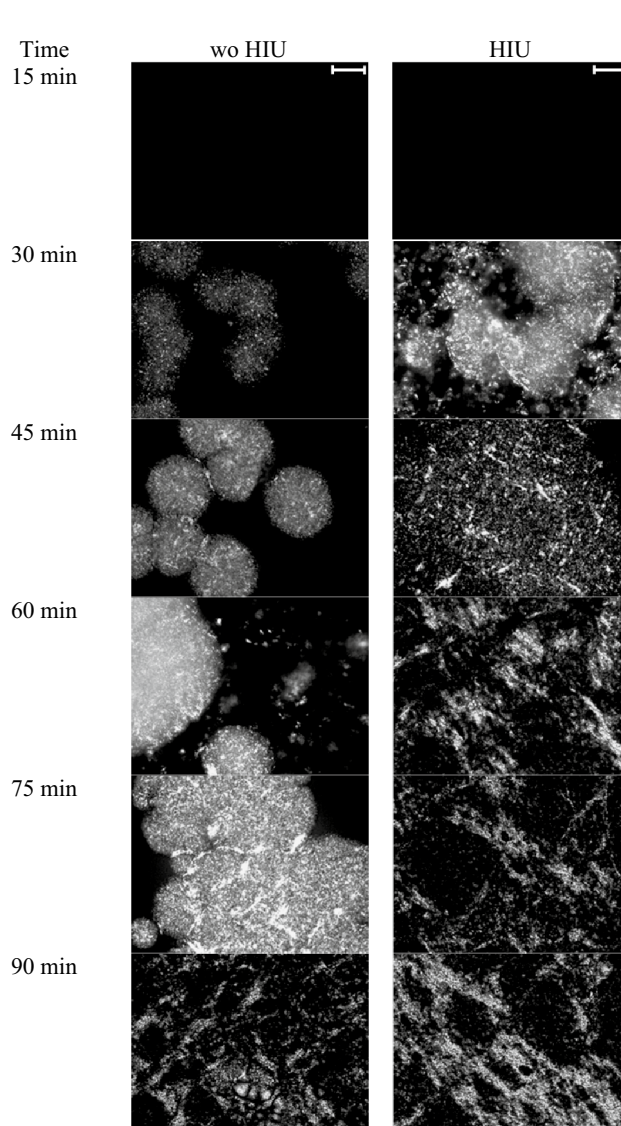
Fig. 6 Polarized-light microscopy (PLM) images of soft stearin crystallized at 21 °C without (wo HIU, *left column*) and with (HIU, *right column*) high-intensity ultrasound pulse. HIU pulse was applied at $t = 17$ min. *White bar* in the first picture of *each column* represents 100 μm

organization at the microscopic level corresponds to a β_1 polymorph.

These results show that HIU was able to significantly change the morphology of the crystals obtained during crystallization. Previous research has shown that HIU induces changes in the morphology of lipid crystals, but most of these changes were associated with crystal sizes and not much with crystal shapes [4–9]. This is the first time that important changes in crystal morphology are obtained as a consequence of sonication. As previously mentioned, based on previous research [16], it is likely that these differences in crystal morphologies are associated with different polymorphic forms.

Melting Behavior

Melting behavior of the samples was evaluated after 120 min at T_c. DSC profiles are shown in Fig. 7, and melting parameters (T_{on}, T_p, and enthalpy) are reported in Fig. 8 for samples crystallized at the different T_c with and without HIU. Melting profiles reported in Fig. 7 show a shoulder at lower temperatures for samples crystallized at 19 and

20 °C without HIU, suggesting the presence of different molecular compounds. These shoulders are more evident in the samples crystallized at 19 °C, but they are not present in the sonicated samples, suggesting that HIU promotes the formation of a more uniform molecular network. Significantly lower T_p ($\alpha = 0.05$) values were observed for the sample crystallized at 19 °C without HIU (Figs. 7a, 8b), which was increased as a consequence of sonication (Figs. 7b, 8b). No significant differences ($\alpha = 0.05$) were observed in the T_{on} values as a function of T_c and sonication (Fig. 8a). The lack of differences observed in general in T_{on} and T_p values between non-sonicated and sonicated samples is somehow unexpected since a different melting profile would have been predicted for the different crystal morphologies obtained in Figs. 2, 3, 4, 5, and 6. This lack of difference can be explained by melting enthalpy values of different polymorphic forms. Rincon-Cardona et al. [16] showed that more stable polymorphic forms of SS have a significantly higher melting enthalpy. It is therefore likely that the melting profile observed in our study is driven by the melting of the most stable polymorphic form (β_1), which is characterized by an agglomeration of crystals

Fig. 7 DSC melting profiles of SS samples crystallized at 17, 18, 19, 20, and 21 °C without (**a**) and with (**b**) HIU
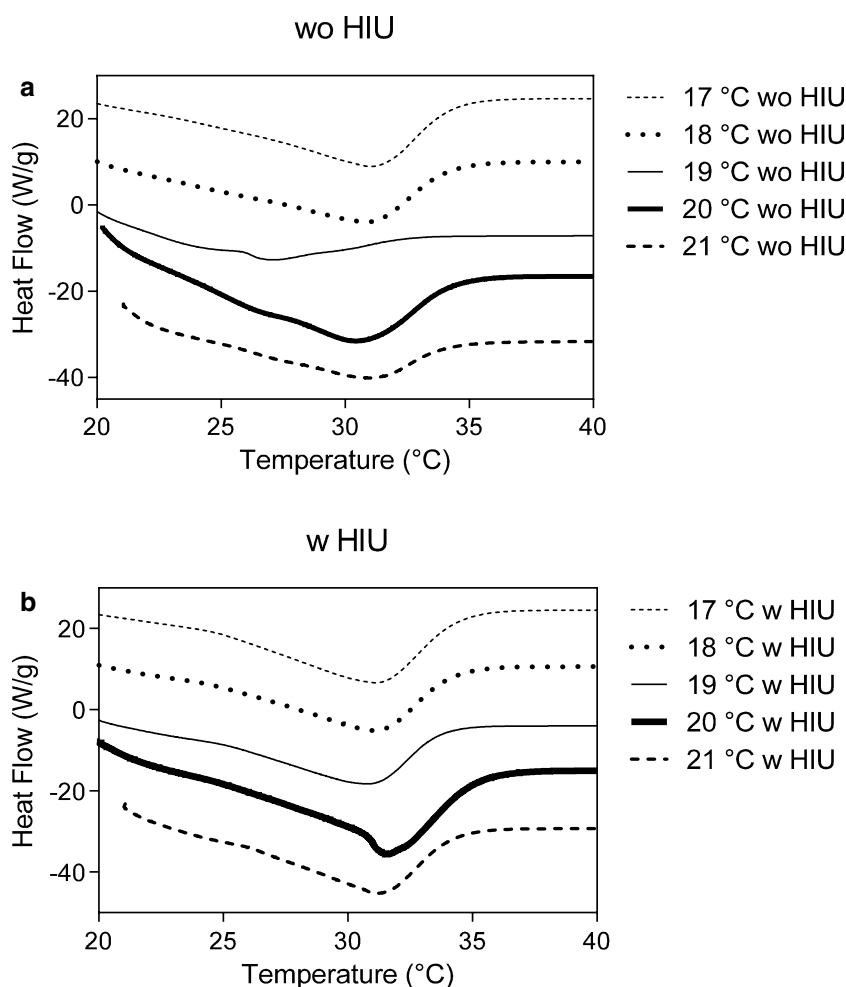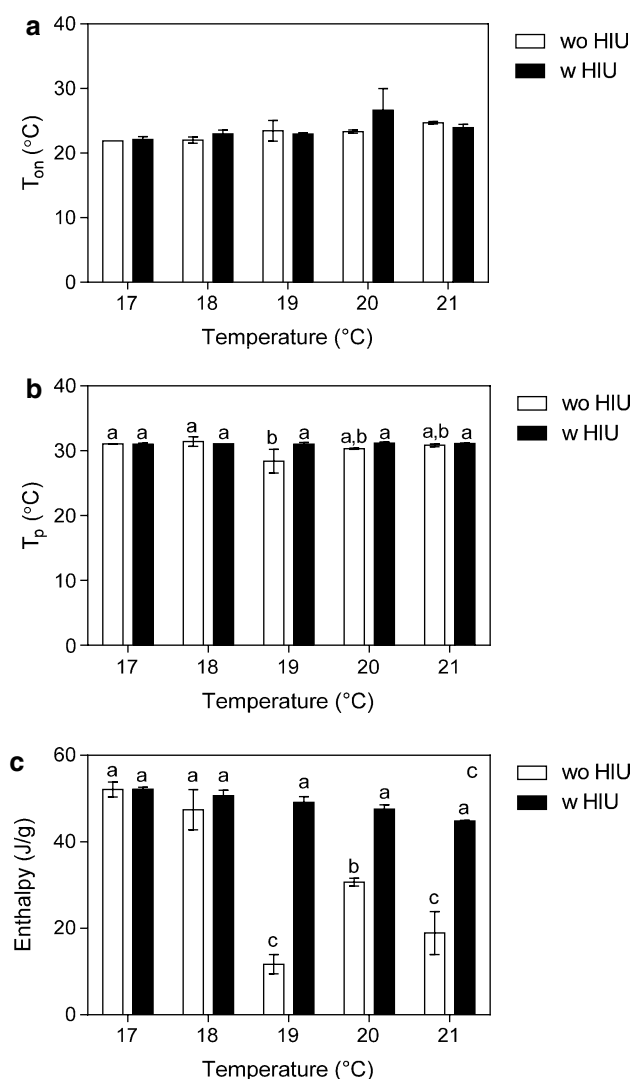
Fig. 8 Melting parameters (T_{on}, T_p, and enthalpy; **a–c**, respectively) for SS crystallized with and without high-intensity ultrasound. Data are expressed as mean values and standard deviations of two replicates. Values with the *same superscripts* indicate that values are not significantly different ($\alpha = 0.05$). T_{on} values were not significantly different ($\alpha = 0.05$)

with no evident microscopic organization (Fig. 2, 3, 4, 5, 6). No significant differences ($\alpha = 0.05$) were found in the enthalpy values of samples crystallized at 17 and 18 °C without HIU, and significantly lower values were observed when samples were crystallized between 19 and 21 °C (Fig. 8c). Enthalpy values of sonicated samples crystallized between 19–21 °C were significantly higher ($\alpha = 0.05$) than those of the non-sonicated counterparts. No significant differences ($\alpha = 0.05$) in enthalpy values were observed as a function of T_c when samples were crystallized in the presence of sonication. Higher enthalpies observed in sonicated samples crystallized at low supercoolings ($T_c = 19$, 20, and 21 °C) might be a result of different factors: (1) the presence of different polymorphic forms, (2) the higher SFC obtained in the sonicated samples at these T_c (Fig. 1), or a combination of both events. These results show that high enthalpy values can be obtained at higher temperatures, for example, 21 °C, when using sonication without the need of increasing the supercooling in the system.

Viscoelastic Properties

The viscoelastic behavior of the samples crystallized at the different temperatures with and without HIU was determined after 120 min into the crystallization process. Table 2 shows the G', G'', and tanδ values. G' and G'' values changed slightly with T_c, with the lowest value obtained at 17 °C. Similarly, the lowest value for tanδ was obtained at 17 °C. Previous research related to fat sonocrystallization describes higher G' values in sonicated samples [8, 9]. Results reported in the present study show an exception to this behavior where lower G', G'' and tanδ values were obtained for the sonicated samples. Considering the SFC values obtained for the sonicated and non-sonicated samples as a function of T_c, we would have expected higher G' values at lower temperatures and for sonicated samples (higher SFC values) at higher crystallization temperatures (19–21 °C); however, this was not the case. It is likely that

Table 2 Storage (G') and loss (G'') moduli, and tanδ values of soft stearin crystallized at different temperatures with and without high-intensity ultrasound pulse

T_c (°C)	G' (×10⁶ Pa)		G'' (×10⁶ Pa)		tanδ	
	wo HIU	HIU	wo HIU	HIU	wo HIU	HIU
17	9.5 ± 0.1[a, c]	9.4 ± 0.2[a, c]	1.3 ± 0.0[a]	1.3 ± 0.1[a]	0.14 ± 0.01[a]	0.14 ± 0.01[a]
18	14.0 ± 0.9[b]	7.8 ± 0.7[a, d]	2.6 ± 0.1[c]	1.2 ± 0.0[a]	0.18 ± 0.01[a]	0.16 ± 0.02[a]
19	12.0 ± 1.7[b, c]	6.9 ± 0.9[a, d]	2.3 ± 0.2[b, c]	1.1 ± 0.1[a]	0.21 ± 0.01[b]	0.16 ± 0.01[a]
20	11.0 ± 2.3[b, c, d]	8.3 ± 0.2[a, d]	2.3 ± 0.1[b, c]	1.4 ± 0.1[a]	0.21 ± 0.03[b]	0.18 ± 0.01[a]
21	13.0 ± 0.7[b, c]	11.0 ± 0.2[b, c, d]	2.0 ± 0.2[b]	1.7 ± 0.1[a, b]	0.17 ± 0.01[a]	0.17 ± 0.01[a]

Data are expressed as mean values and standard deviations of two replicates. Data with the same superscript are not significantly different ($\alpha < 0.05$)

this lower level of viscoelasticity obtained as a consequence of sonication is due to the different crystal morphologies and/or polymorphic forms obtained in the systems.

Conclusion

This research showed that HIU can be used to induce and increase the rate of crystallization of a soft stearin obtained from a high-stearic high-oleic sunflower oil fraction. In addition, HIU significantly changed the morphology of the crystals formed, increased the amount of SFC and enthalpy values, and changed the melting behavior of the samples, especially when samples were crystallized at high T_c. These findings show that HIU can be used with other processing conditions to change the crystallization properties and functionality of lipids. This research demonstrated that HIU can be used to process fats at lower supercoolings while maintaining physical properties obtained at higher supercoolings.

References

1. Patist A, Bates D (2008) Ultrasonic innovations in the food industry: from the laboratory to commercial production. Innov Food Sci Emerg 9:147–154
2. Soria AC, Villamiel M (2010) Effect of ultrasound on the technological properties and bioactivity of food: a review. Trends Food Sci Tech 21:323–331
3. Patrick M, Blindt R, Janssen J (2004) The effect of ultrasonic intensity on the crystal structure of palm oil. Ultrason Sonochem 11:251–255
4. Chen F, Zhang H, Sun X, Wang X, Xu X (2013) Effects of ultrasonic parameters on the crystallization behavior of palm oil. J Am Oil Chem Soc 90:941–949
5. Martini S, Suzuki AH, Hartel RW (2008) Effect of high intensity ultrasound on crystallization behavior of anhydrous milk fat. J Am Oil Chem Soc 86:621–628
6. Suzuki AH, Lee J, Padilla SG, Martini S (2010) Altering functional properties of fats using power ultrasound. J Food Sci 75:208–214
7. Wagh A, Walsh MK, Martini S (2013) Effect of lactose monolaurate and high intensity ultrasound on crystallization behavior of anhydrous milk fat. J Am Oil Chem Soc 90:977–987
8. Ye Y, Wagh A, Martini S (2011) Using high intensity ultrasound as a tool to change the functional properties of interesterified soybean oil. J Agric Food Chem 59:10712–10722
9. Ye Y, Tan CY, Kim D, Martini S (2014) Application of high intensity ultrasound to a zero-trans shortening during temperature cycling under different cooling rates. J Am Oil Chem Soc 91:1155–1169
10. Higaki K, Ueno S, Koyano T, Sato K (2001) Effects of ultrasonic irradiation on crystallization behavior of tripalmitoylglycerol and cocoa butter. J Am Oil Chem Soc 78:513–518
11. Dubisnky E, Garcés R (2011) High-stearic/high-oleic sunflower oil: a versatile fat for food applications. INFORM 22:369–372
12. Fernández-Moya V, Martínez-Force E, Garcés R (2005) Oils from improved high stearic acid sunflower seeds. J Agric Food Chem 53:5326–5330
13. Bootello MA, Garcés R, Martínez-Force E, Salas JJ (2011) Dry fractionation and crystallization kinetics of high-oleic high-stearic sunflower oil. J Am Oil Chem Soc 88:1511–1519
14. Salas JJ, Bootello MA, Martínez-Force E, Garcés R (2011) Production of stearate-rich butters by solvent fractionation of high stearic–high oleic sunflower oil. Food Chem 124:450–458
15. Bootello MA, Hartel RW, Garcés R, Martínez-Force E, Salas JJ (2012) Evaluation of high oleic–high stearic sunflower hard stearins for cocoa butter equivalent formulation. Food Chem 134:1409–1417
16. Rincón-Cardona JA, Martini S, Candal RJ, Herrera ML (2013) Polymorphic behavior during isothermal crystallization of high stearic high oleic sunflower oil stearins. Food Res Int 51:86–97
17. Martini S, Rincón-Cardona JA, Ye Y, Candal RJ, Herrera ML (2013) Crystallization behavior of high-oleic high-stearic sunflower oil stearins under dynamic and static conditions. J Am Oil Chem Soc 90:1773–1786
18. Rincón-Cardona JA, Agudelo-Laverde LM, Martini S, Candal RJ, Herrera ML (2014) In situ synchrotron radiation X-ray scattering study on the effect of a stearic sucrose ester on polymorphic behavior of a new sunflower oil variety. Food Res Int 64:9–17
19. Campos R (2005) Experimental methodology. In: Marangoni AG (ed) Dekker fat crystal networks. Marcel Dekker, New York, pp 267–348
20. Leighton TG (ed) (1994) Chapter 1: The sound field. In: The acoustic bubble. Academic Press, New York, pp 1–66
21. Martini S, Tejeda-Pichardo R, Ye Y, Padilla SG, Shen FK, Doyle T (2012) Bubble and crystal formation in lipid systems during high-intensity insonation. J Am Oil Chem Soc 89:1921–1928